M. Elgezzar
Researcher
Department of Mechanical Power & Energy
Military Technical College, Cairo
Egypt

A. Rashad
Associate Professor
Department of Mechanical Power & Energy
Military Technical College, Cairo
Egypt

M. S. Hassan
Associate Professor
Department of Mechanical Power & Energy
Military Technical College, Cairo
Egypt

T. Elnady
Assistant Professor
Department of Mechanical Power & Energy
Military Technical College, Cairo
Egypt

CFD Analysis and Geometrical Parameter Investigation For The Design of A High-Efficiency Supersonic Ejector

This paper presents a CFD analysis of a supersonic ejector model for refrigeration systems. The model is validated by comparing it with previous studies and used to design a high-efficiency ejector. The effects of geometrical parameters such as convergence angle, throat length, divergence angle, and diffuser length on the entrainment ratio are studied. The optimal values of these parameters are found and used to modify the base model. The performance of the optimized model is evaluated under different operating conditions. The paper aims to provide design guidelines for supersonic ejectors in refrigeration applications

.

Keywords: *Supersonic ejector, Nozzle, CFD modeling, Entrainment ratio, Refrigeration, Ejector geometry, Performance Evaluation.*

1. INTRODUCTION

Supersonic ejectors can be considered the simplest mechanical components in comparison with vacuum pumps and compressors, as they lack any moving mec–hanical parts and don't need lubricants to achieve the recompression and the mixing of the two overlapping fluid streams. Moreover, its ability to utilize low-tem–perature heat to produce cooling makes ejector refri–geration a promising solution for economical and environmentally safe technologies and makes it attrac–tive for the industrial and automotive fields in waste-heat recovery appliances.

A long time ago, ejectors for compressible fluids were recognized and used in a variety of technical applications. In aeronautical engineering, they can be used to evaluate a propulsion system's altitude by lowe–ring the pressure in a test chamber [1]. In order to decrease the thermal signature, exhaust gases and fresh air are mixed using the pumping effect [2].

The utilization of supersonic ejectors for refrige–ration systems is the major focus of this paper. Undoub–tedly, it is one of the most significant applications for ejectors, according to numerous papers available on this subject.

The review papers by [3] and [4] provide a decent overview of the various applications in this topic, which piqued the interest of many experts in an effort to develop energy-efficient and eco-friendly techniques in reaction to present practices that are causing environ–mental damage such as ozone depletion and global war–ming. [5] Present and categorize a review of solar-driven ejectors used in refrigeration systems, a develop–ment history, and improvements to ejector refrigeration systems. [6] and [7] Provided an overview of ejector refrigeration systems' historical and present impro–vements.

Work shown in [8] provides recent advancements in ejector refrigeration technology, reporting and catego–rizing a wide range of studies on topics such as geo–metric optimization, mathematical simulations, refrige–rant selection, and operating condition optimization.

Many experimental and theoretical investigations have been conducted to understand better not just the fundamental mechanisms of heat transfer and fluid dynamics but also the operational behavior of the ejectors.

Early studies were based on one-dimensional mo–dels. [9] Set up a one-dimensional (1-D) model using air as a working fluid, and then [10] used refrigerants as a working fluid. These one-dimensional models provided a general understanding of ejectors, but they were unable to understand the flow physics that locally occurs along with the ejector, such as local interactions between boundary layers and shock waves and their influence on the recompression and mixing rate. A better understanding of this physics would allow a more accurate and reliable design.

The effect of different turbulence models on the simulation results using air as a working fluid was studied in [11], whereas [12] used refrigerant R142b and described its thermophysical properties using real properties rather than ideal gas properties. In [13], refrigerant R141b was used, as well as R236fa and R245fa as the working fluid and it was found that using standard k-epsilon as a turbulence model yielded good results during the simulation. Paper [14] investigated numerically Different shock generation and reflections in different types of supersonic nozzles.

Paper [15] studied the effect of shock wave struc-tures on the ejector performance using nitrogen as the operating fluid and discovered that the pressure-based RNG k-ε model gave the best predictions of both the structures of shock waves and the mass flow rate. Paper [16] accounted for the real properties of R245fa refri–gerant in the simulations using a density-based k-ω-SST turbulence model and recommended defining the ejector

Received: August 2023, Accepted: October 2023
Correspondence to: Mr.Mahmoud Elgezzar
Military Technical College,
Ismail Al Fangari, El-Qobba Bridge, Cairo, Egypt.
E-mail: mahmoud.elgezzar@gmail.com
doi: 10.5937/fme2401011E

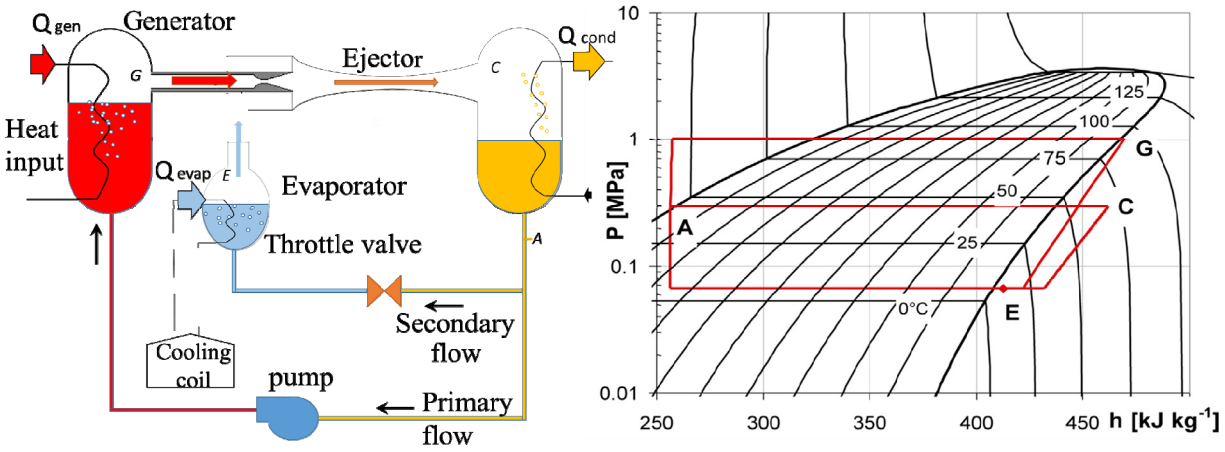

Figure 1: Schematic view of the thermodynamic cycle and the refrigeration system using ejector

surface roughness accurately. The effect of geometric parameters on ejector performance has been investi–gated numerically and experimentally in many types of research. Paper [17] used the CFD to study the optimi-zation of high-efficiency ejectors and provided Several earlier studies where a number of researchers attemp-ted to understand how the ejector geometry affected the performance of the jet ejector and [18] Studied the Effects of suction chamber geometry and provided a decent review of previous work that concerned with the study of the Effects of various operating conditions on the ejector performance, such as nozzle velocity, pressure drop, and ejector geometry parameters.

After that [19] studied the effects of changing the converging angle of the mixing section and the position of the primary nozzle exit on the ejector performance and found that increasing the primary flow pressure causes the optimum converging angle and the optimum position of the primary nozzle exit to increase.

[20] Studied the effects of different geometries of the primary nozzle on the performance of a steam ejector used in the refrigeration cycle, using a density-based k-omega-SST turbulence model to explain flow inside the ejector. Also, [21] and [22] studied the supersonic flow of air through a 2D nozzle Using a density-based k-ω SST turbulent model, which agreed well with experimental results.

[23] studied the influences of the mixing chamber and the diffuser section lengths on the performance of the CRMC ejector. [24] studied the effect of the Throat length on the Flow Patterns in supersonic nozzles Using the Spalart-Allmaras.[25] used the SST k-turbulence model with air as a working fluid to study the effect of jet nozzle geometry on supersonic ejector performance.

From the review, it could be concluded that many researchers studied the effect of the geometrical parameters for ejectors work with steam and R245. To the best of our knowledge, the work done on supersonic ejectors in refrigeration cycles using R142b had a little cover in research. The current work aims to investigate the influence of different geometrical parameters on the performance of this type of ejector. According to the literature review, an effective ejector performance optimization method requires geometric optimization under specific operating conditions. In this paper, diffe-rent turbulence models using R141b as the working fluid were tried to investigate the performance of a supersonic ejector used in refrigeration applications. The CFD model validation is first presented, then the influence of different geometrical parameters on the ejector per–formance is discussed to determine the suitable mec-hanisms that contribute to improving ejector performance and to design a high-efficiency supersonic ejector.

1.1 Supersonic ejector in a refrigeration cycle

The schematic drawing in Fig 1 illustrates a thermo-dynamic cycle of a supersonic ejector operating in one of the simplest forms of a refrigeration cycle. In this cycle, a supersonic ejector, vapor generator, and liquid feed pump replace the mechanical compressor. The primary fluid with the highest total energy from the generator is the motive one, while the other with the lowest total energy from the evaporator is the secondary or induced stream.

During regular operation of such systems, the primary fluid is accelerated to supersonic speed as it passes through a converging-diverging nozzle. This low-pressure primary flow exits the nozzle and entrains and accelerates the secondary fluid stream from the evaporator by an entertainment-induced effect.

The two streams interact and enter the mixing chamber, where they are re-compressed and mixed. Complicated interactions occur between the mixing layer and shocks. This indicates that there is a transfer of energy from the greatest energy level to the lowest energy level, with a mixing pressure value located between the driving pressure and induction pressure.

After the two streams are mixed, a series of shock waves occur, which reduce the flow velocity to subsonic speeds. The resulting subsonic flow and shock waves through the diffuser cause the flow pressure to increase to match that at the condenser at point C. After the condenser, there are two currents: one is returned to the generator via a feed pump, while the other is expanded to the evaporator through a throttling valve.

1.2 Ejector theory

An important variable to express the performance of a supersonic ejector is the entrainment ratio, which can be expressed as the ratio between the secondary mass flow rate and the primary mass flow rate as in (1).

$$ER = \frac{\text{mass flow of entrained flow}}{\text{mass flow of primary flow}} = \frac{m_{\dot{e}}}{m_{\dot{g}}} \quad (1)$$

Hence, the performance of the refrigeration system can be determined by means of the Coefficient of Performance (COP), which can be defined by dividing the cooling load by the total power and heat inputs.

$$cop = \frac{Q'_{evp}}{W_{pump} + Q'_{gen}} = \frac{m_{\dot{e}}}{m_{\dot{g}}} \frac{h_{g-evp} - h_{f-con}}{h_{g-gen} - h_{f-con}} \quad (2)$$

$$ER = \frac{m_{\dot{e}}}{m_{\dot{g}}} \quad (3)$$

$$cop = ER \frac{h_{g-evp} - h_{f-con}}{h_{g-gen} - h_{f-con}} \quad (4)$$

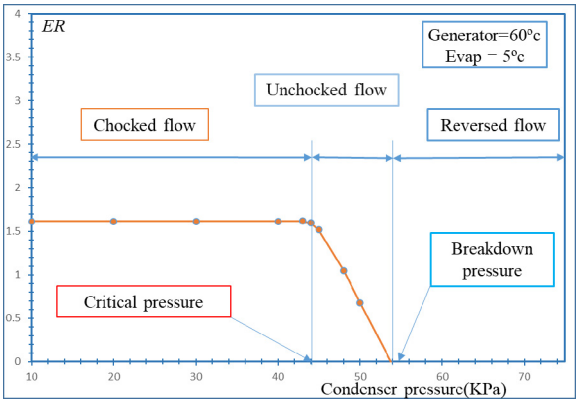

Figure 2: Effect of changing the condenser pressures on the ejector performance acquired through CFD simulation for a generator temperature of 60°c and an evaporator temperature of 5°C

As shown in (4), the performance of the refri–ge–ration system depends largely on the Entrainment Ratio.

During operation, it's found that by increasing the ejector back pressure (condenser pressure) for the same evaporator and generator pressures, the value of the entrainment ratio remains invariable until a critical back pressure (condenser pressure) (pc^*) is reached. Incre–asing condenser pressure above that critical pressure causes the entrainment ratio to drop rapidly until the ejector ceases to operate.

As illustrated in Fig 2, The ejector's performance curve is separated into three regimes: the critical (choked flow) regime, the subcritical (unchoked flow) regime, and the backflow (reversed flow) regime. As shown in the curve, a point called "critical condenser pressure" separates between the choked flow and the unchoked flow regions, and a point called "breakdown backpressure" separates between the reversed flow and the unchoked flow regions.

For the critical (choked flow) regime, the pressure of the condenser is below the critical value. The quantity of the secondary entrained fluid drawn from the evaporator is constant, which leads to a constant value of the entrainment ratio. In this mode, after the nozzle, the primary fluid expands, presenting a series of oblique shocks in the suction chamber and accelerating the secondary fluid to choke in the mixing chamber; then, in the diffuser, the mixed flow shocks again, which is known as a double choking phenomenon [10]. The location of the shock in the mixing chamber depends on the condenser pressure. When the condenser pressure is increased, the oblique shock will shift upstream (toward the primary nozzle) without making any disturbance to the mixing process, as shown in Fig 3.

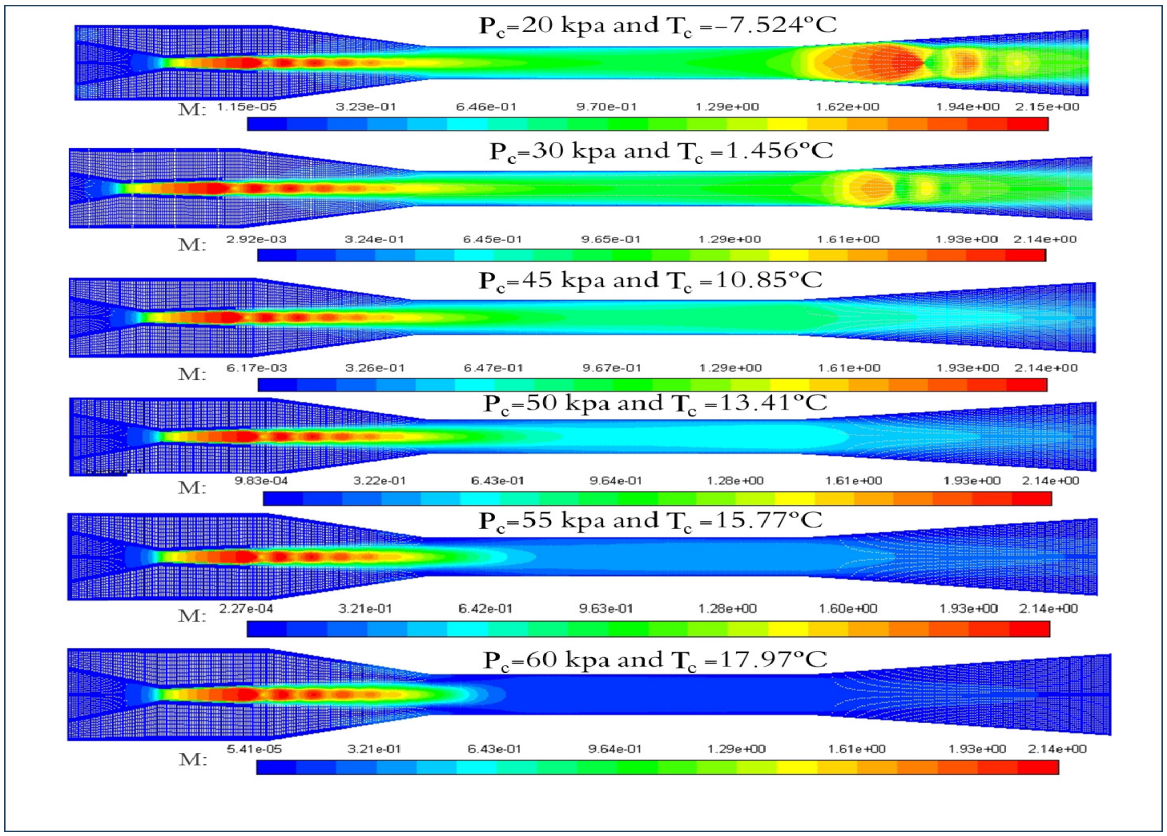

Figure 3: Mach number contours illustrate the oblique shock motion as the condenser pressure increases

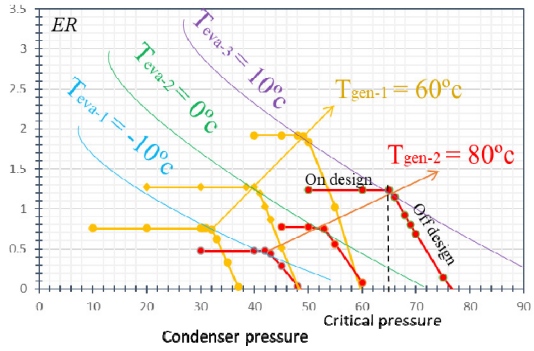

Figure 4: An example of the ejector operation curve at different evaporator and generator inlet conditions

For the subcritical (unchoked flow) regime, the ejector's condenser pressure is greater than the critical value. When the condenser pressure is increased above that critical pressure, the value of the entrainment ratio remarkably drops.

In the diffuser, the flow does not reach the choking condition (single-choking) [10]. The choking of the flow no longer occurs in the mixing chamber. The oblique shock is thought to move upstream into the converging duct section and leads to disturbance in the mixing process between the primary fluid and the entrained fluid.

For the backflow (reversed flow) regime, the condenser pressure is higher than the breakdown value. In this region, the mixed flow direction is reversed back to the secondary flow inlet, and then the ejector finally malfunctions.

Changing the generator and evaporator conditions causes significant modifications in the entrainment ratio and the critical pressure. As shown in Fig 4, rising evaporator temperature (from $T_{eva\text{-}1}$ = -10°c to $T_{eva\text{-}3}$ =10°c) leads to greater values of the entrainment ratio (due to the greater amount of secondary mass flux) and critical pressures (as a result of the increase in the total pressure of the entrained flow). But when the generator temperature is (from $T_{gen\text{-}1}$ =60°c to $T_{gen\text{-}2}$ =80°c), the entrainment ratio is reduced as the increase in the primary mass flow is not followed by an increase in the entrainment of the secondary stream, whose mass flow rate stays almost constant [11]. However, the larger the amount of energy content introduced by the primary flow, the higher the condenser (back) pressures and the critical pressure.

2. THE SUPERSONIC EJECTOR CFD MODEL SETUP

The CFD technique depends on two main functions: creating and preparing the physical model (domain of calculation) and solving the resulting set of mathematical equations. In this study, a commercially available CFD package fluent 18.2 has been used to form and solve a two-dimensional, axis-symmetric model.

The ejector with its general schematic drawing is created, as shown in Fig 5.

The geometry was designed in 2D, where it is assumed that the supersonic ejectors are axis-symmetric, and only the top half of the ejector was modeled and created, as shown in Fig 6.

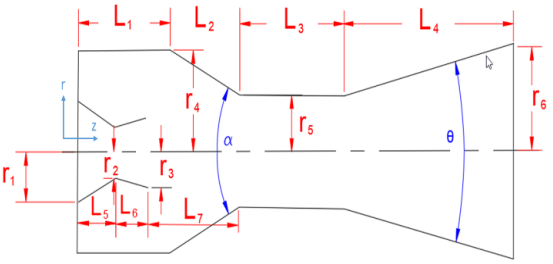

Figure 5: Ejector geometry

Figure 6: Geometry made on Design Modeller

In Figure 7, after the geometry, the model was meshed, and named selections were made for one primary stream inlet, one secondary stream inlet, and the ejector outlet. The first layer size at the direction normal to the wall was at first assumed, then from CFD results using post-processor, the y^+ value was extracted. In the first trial, the y^+ value at the wall was high (between 5 and 22), and according to ([26], [27]), it is recommended to get a y^+ value less than 5. Therefore, the cell near the wall is refined using the adaptation technique until we have the desired y^+ values. The variation of y^+ values during refinement on the ejector wall, the inside wall of the nozzle, and the outside wall of the nozzle is shown in Fig 8, Fig 9 and Fig 10.

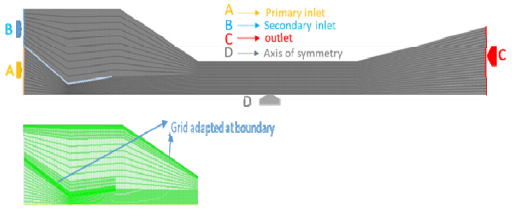

Figure 7: Example of the base grid for domain discretization

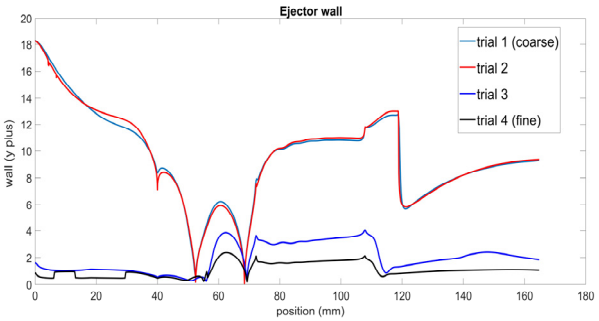

Figure 8: The behavior of y+ in the ejector wall

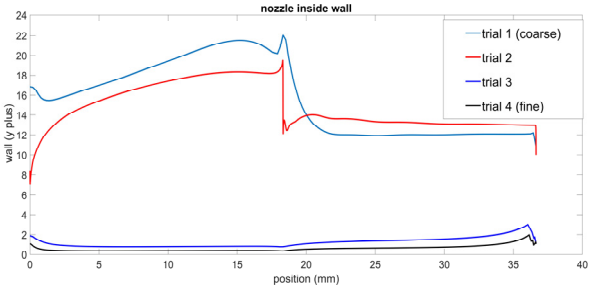

Figure 9: The behavior of y+ in the inside wall of the nozzle

The grid independence was analyzed by comparing the results of different meshes using the Realizable k-ε model. The grid independence check was performed on the model of geometry AB (refer to Table 2) and the inlet boundary conditions as model AB1(refer to Table 3) and an outlet pressure of 0.06 MPa. The results showed (refer to Table 1) that there are only slight changes in the entrainment ratio beyond 33,000 cells. So, for further study, a cell number of around 33,000 has been used.

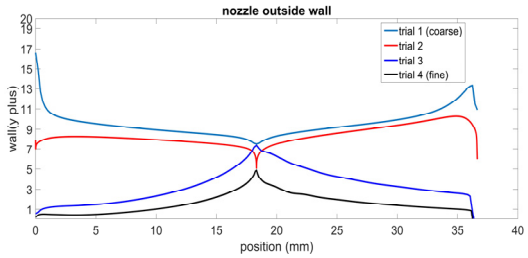

Figure 10: The behavior of y+ in the outside wall of the nozzle

Table 1: Grid independence study

Model No	No. of cell	Entrainment ratio (*ER*)
M-1	2518	0.3905
M-2	4442	0.3895
M-3	6982	0.3901
M-4	9936	0.3910
M-5	16590	0.3945
M-6	33050	0.3935
M-7	96409	0.3935
M-8	191526	0.3935

2.1 Model Governing equations

The fluid flow within the ejector is governed by a steady-state two-dimensional compressible form of the fluid flow conservation equations where derivatives with respect to time can be neglected.

As a result, the governing equations can be expres–sed as follows in their compact Cartesian form:

$$\frac{\partial u_i}{\partial x_i} = 0 \tag{5}$$

$$\frac{\partial \rho u_i u_j}{\partial x_i} = \frac{\partial P}{\partial x_i} + \frac{\partial \tau_{ij}}{\partial x_j} \tag{6}$$

$$\frac{\partial}{\partial x_i}\left(u_i\left(\rho E + P\right)\right) = \nabla\left(\lambda \frac{\partial T}{\partial x_i} + u_i \tau_{ij}\right) + S_h \tag{7}$$

where E is the total energy ($E = h + u^2/2 - P/\rho$) and S_h is the source term.

2.2 Numerical modeling

Ansys fluent 18.2 workbench package was used for solving, pre-processing, and post-processing this comp–ressible fluid. The geometry was created in Design Mo–deler and divided into grid elements in Ansys meshing.

The non-linear governing equations were solved with the trial of using the pressure-based and implicit density-based solvers using the model of the ideal gas and three turbulence models: Realizable k-ε model, Standard k-ε model, Renormalization-group (RNG) k-ε model (for both pressure and density-based solver) were tested in order to solve the high-speed supersonic flow within the ejector.

Table 2: Geometry used in the model validation from [10]

	Radii (mm)						Lengths (mm)					
	r_1	r_2	r_3	r_4	r_5	r_6	l_2	l_3	l_4	l_5	l_6	l_7
AG	6.65	1.32	2.25	11.55	3.76	7.04	32.24	35.6	56.94	18.32	18.32	35.6
AB	6.65	1.32	2.25	11.55	3.49	7.04	32.24	35.6	56.94	18.32	18.32	35.6

Table 3: A list of the ejector's operating conditions and different model results for the ejectors

Model	P_g [Mpa]	T_g [°C]	P_e [Mpa]	T_e [°C]	*E.R.* CFD[2] [err %]	*E.R.* Exp[1]	*E.R.* 1D[1] [err%]	*E.R.* [error %]					
								Density-based			Pressure based		
								Standard	Realizable	RNG	standard	Realizable	RNG
AB1	0.400	78	0.0399	8	0.3982 [1.53%]	0.392	0.4422 [12.8%]	0.3766 [-3.9%]	0.4138 [5.49%]	0.3808 [-2.9%]	0.3420 [12.8%]	0.3936 [0.35%]	0.3555 [-9.4%]
AB2	0.465	84	0.0399	8	0.3266 [4.78%]	0.311	0.3042 [-2.4%]	0.3051 [-2.1%]	0.3377 [8.34%]	0.3082 [-1.1%]	0.2567 [-18%]	0.3155 [1.21%]	0.2722 [-12.8%]
AB3	0.538	90	0.0399	8	0.2673 [-1.66%]	0.271	0.2093 [-22.9%]	0.2154 [-21%]	0.2607 [-4.07%]	0.2270 [-17%]	0.1852 [-32%]	0.2592 [-4.84%]	0.2040 [-24.9%]
AG1	0.400	78	0.0399	8	0.4712 [7.26%]	0.439	0.4609 [4.92%]	0.4806 [9.39%]	0.5033 [14.57%]	0.4784 [8.9%]	0.4473 [1.83%]	0.4794 [8.37%]	0.4508 [2.63%]
AG2	0.465	84	0.0399	8	0.3986 [2.65%]	0.388	0.3704 [-4.61%]	0.3939 [1.44%]	0.4154 [6.98%]	0.3936 [1.4%]	0.3522 [-9.2%]	0.3914 [0.78%]	0.3579 [-7.8%]
AG3	0.538	90	0.0399	8	0.3319 [9.18%]	0.304	0.2395 [-21.2%]	0.3017 [-0.8%]	0.3305 [8.73%]	0.3060 [0.7%]	0.2747 [-9.7%]	0.3055 [0.48%]	0.2783 [-8.5%]
AG4	0.604	95	0.0399	8	0.2821 [10.54%]	0.255	0.2144 [-15.9%]	0.2235 [-12%]	0.2618 [2.60%]	0.2372 [-7.1%]	0.2111 [-17%]	0.2596 [1.70%]	0.2171 [-15%]
AG5	0.400	78	0.0472	12	0.5834 [-4.86%]	0.613	0.6659 [8.59%]	0.5604 [-8.6%]	0.6129 [-0.06%]	0.5702 [-7.0%]	0.5203 [-15%]	0.5951 [-3%]	0.5336 [-13%]
AG6	0.465	84	0.0472	12	0.4893 [2.15%]	0.479	0.4769 [-0.44%]	0.5120 [6.89%]	0.5178 [8.09%]	0.4697 [-1.9%]	0.4769 [-0.4%]	0.4949 [3.2%]	0.4730 [-1.3%]
AG7	0.53	90	0.0472	12	0.4093 [1.46%]	0.403	0.4142 [2.68%]	0.3841 [-4.8%]	0.4333 [7.41%]	0.4461 [10.6%]	0.3771 [-6.5%]	0.4108 [1.81%]	0.3809 [-5.6%]
AG8	0.604	95	0.0472	12	0.3505 [0.06%]	0.350	0.3434 [-1.97%]	0.3239 [-7.5%]	0.3653 [4.27%]	0.3530 [0.8%]	0.3132 [-11%]	0.3367 [-4.04%]	0.3163 [-9.7%]

[1] (Huang et al., 1999) [10] Results. [2] (D. Scott et al., 2008) [22] Results.

The second-order upwind scheme was used to discretize the convective terms. For the pressure field, the coupled algorithm was applied. The scalable wall function was employed for the near-wall treatment. The model's working fluid was R141b, with the use of the EES (Engineering Equation Solver pro 9) database to calculate the thermophysical properties of R141b. The ideal gas relationship was used to determine the fluid density. The viscosity, thermal conductivity, and specific heat were assumed to remain constant over the whole solution domain.

2.3 Model Geometry and Operating Boundary Conditions

The CFD model's geometry was first set to simulate the AG and AB geometries of [10]. The primary and secondary inlet boundary conditions were considered as pressure inlets and their pressure values were taken as the saturation pressure of the corresponding temperature taken directly from [10] (refer to Table 3); the outlet boundary condition was considered as a pressure outlet of 0.06 MP and a corresponding saturation temperature of 17.79 °C. Table 2 provides an overview of the geometry using (Fig 5) as a guide.

For all solid surfaces in the model, the no-slip boundary condition was used. The z-axis was a symmetry axis. Table 3 summarizes the operating conditions, reference results, and CFD results for different turbulence models.

2.4 Model validation

The proposed model was validated by comparing its results with those of [10] and [28], which included experimental studies and one-dimensional and two-dimensional axis-symmetric CFD models of supersonic ejectors. For all geometries and ejector models used in this study, a comparison between the numerically calculated and experimentally measured entrainment ratios is shown in Table 3. In comparison with the experimental results, the pressure-based Realizable k-ε model was the best suited to predict the entrainment ratio, which agrees with [29], which states the ability of the realizable k-ε model to accurately predict the spreading rate of both curved and planar jets and its ability to provide excellent performance for flows that involve boundary layers subjected to strong adverse pressure gradients and separation.

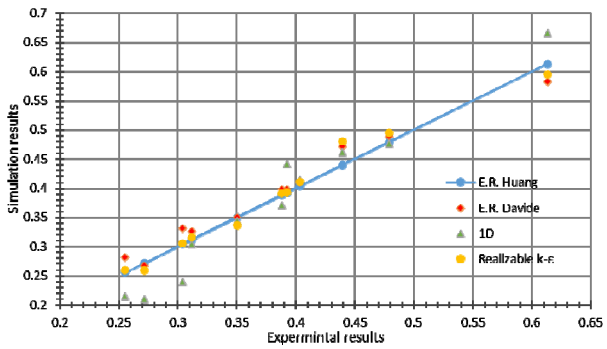

Figure 11: Entrainment ratios from (Huang et al., 1999) [10] compared to those from other models

Also, Table 3 and Fig 11 show the 1D model results of [10] and the CFD model results of [28]. The solid line shows a complete correlation between the modeling and experimental data. The results of the CFD models are shown as points. The points closest to the solid line represent a better comparison.

The differences in entrainment ratios between the experimental and predicted results of the pressure-based Realizable k-ε model are between -4.8% and 8.4%; for the 1-D simulation of [10], the differences range from -22.9% to 12.8%; and for the CFD results of [28], the differences range from -4.9% to 10.6%. The suggested model is, therefore, comparable to that of [28].

3. RESULTS AND DISCUSSION

CFD techniques were used to determine the optimal geometry and operating conditions for the design of a high-efficiency jet ejector. The geometrical parameters that affect performance, such as angle of convergence, throat section length, and diffuser section, have been studied. The variation of the entrainment ratio of the ejector was computed independently based on the new geometry design conditions of the ejector. Only one dimension of the concerned geometrical parameter was changed at each time to study its effect on the ejector performance.

Table 4: Ejector dimensions used by previous investigators from (R. L. Yadav & Patwardhan, 2008).

References	Angle of converging Section α	Throat aspect ratio $l_3/2r_5$	Angle of diverging section θ
(Bhat et al., 1972) [34]	28	0	10
(Zahradnik et al., 1982) [35]	-	0	6.4
(Moresi et al., 1983) [36]	17.35	1.8	9.5
(Brahim et al., 1983) [37]	-	3.5	2
(Bhutada et al., 1987) [38]	12	0: 16	5
(Kundu et al., 1994) [39]	-	7	7
(Havelka et al., 1997) [40]	-	5: 20	7
(Cramers et al., 2001) [41]	-	2: 10	3
(Elgozali et al., 2002) [42]	-	10	7
(Gamisans et al., 2004) [43]	-	10	-
(Rusly et al., 2005) [44]	10	0.5:1.3	7
(Li & Christofides, 2005) [45]	12	5	2

Paper [17] Provided some optimum dimension values for different ejector components suggested by different investigators, such as:

For the convergence section, according to [30], an angle greater than 20 degrees is recommended for a conical or tapered entrance, as the nozzle jet that has a typical angle of around 20 degrees will not generate objectionable shock and eddy losses at the convergence entrance. Moreover, [31] discovered that the best convergence angle is about 25 degrees.

For the throat section, according to [32], its length must be accurately designed. It should be long enough to generate a uniform velocity profile before the divergence section entrance, as the uniform velocity reduces the energy losses in the divergence section; thus, a better

pressure recovery is obtained. The opti–mum length for the throat section, according to two literature studies cited in [32] and [9], is around 7 times the throat diameter. On the other hand, [33] proposed a different optimum length of 7.5 times the throat diameter.

For the divergence section, according to [32], it is not recommended to have an excessively rapid diver–gence after the throat section, and it indicated that an angle θ for the divergent section is recommended to have a range of 4 to 10 degrees. For better pressure recovery, its length is recommended to be from 4 to 8 times the throat diameter.

While [18] provided some of the optimum dimen–sion values of components of conical ejectors suggested by previous investigators compiled in Table 4.

For the throat section, according to [46], the opti–mum ratio between throat section length and diameter is between 7 and 10. And according to other publications given in references ([47-51]), the optimum ratio between throat section length and diameter is between 7 and 11.

For the divergence section, according to ([52]; [53]), the optimal diffuser angle of divergence for vapor and steam ejectors is 5 to 7 degrees.

Taking the validated model AB1 from Table 3 as a case study and changing its dimensions according to the above recommendation by taking the convergence angle to be 25 degrees, the throat length to be 7.5 times the throat diameter ($l_3 /2r_5 = 7.5$), the divergence angle θ to be 10 degrees, and the divergence section length to be 6 times the throat diameter ($l_4/2r_5 = 6$). The optimized dimensions of this geometof Fig 5) are showry (refer to the schematic illustration n in Table 5, and it was found that the 'entrainment ratio' increased from 0.3935 to 0.8548. Then, a parametric study was performed on this model (Opti-1) for more performance enhancement.

3.1 Effect of the angle of the convergent section

The effect of changing the convergence angle α on the entrainment ratio was numerically predicted using the validated model at the on-design condition by changing the angle α (as shown in Table 5) from (18°: 28°) and as shown in Fig 12 the maximum value of entrainment ratio is achieved at a convergence angle of α =23°

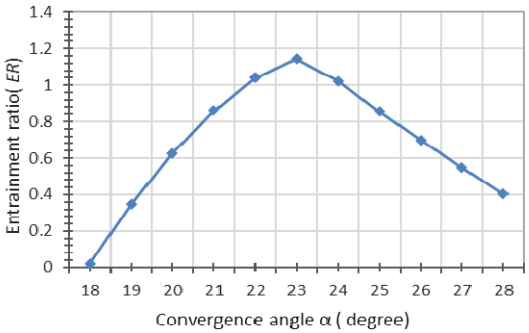

Figure 12: Effect of convergence angle on Entrainment ratio

. The variation in convergence angle below or above that value decreases the ejector's entrainment ratio.

3.2 Effect of throat section length

The mixing section of the ejector system is a critical geometrical component that is subjected to substantial shock trains as a result of the intensive interaction between the supersonic primary flow and the subsonic entrained flow**.** According to several literature sources, the ejector mixing length should be 7 to 9 times the throat diameter for the best performance of the ejector.

According to [33], any mixing length between 4 and 14 throat diameters will provide around 4% of optimum performance. From Table 5, to study the effect of the mixing length on the entrainment ratio, the value of the ratio ($l_3 /2r_5$) was changed from (4:10); this effect was shown in Fig 9 for different convergence angles, where the results showed that the maximum entertainment ratio was achieved at ($l_3 /2r_5 = 4$).

3.3 Effect of angle and length of the divergent section

The diffuser section of the ejector converts the momentum and kinetic energy of the incoming mixture from the mixing section into pressure energy. It allows a higher pressure discharge from the ejector system than the suction pressure. The entrainment ratio at different divergence angles ($\theta = 4°:20°$) was numerically predicted at the on-design condition to investigate the divergence angle effect on the ejector performance.

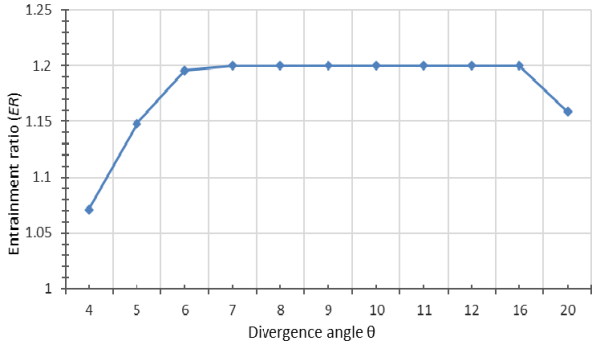

Figure 131: Effect of divergence angle on Entrainment ratio

The effect of the divergence angle on the entrai–nment ratio is shown in Fig 13. The results showed that the entrainment ratio is constant from ($\theta = 7°:16°$). The variation in diffuser angle below or above decreases the entrainment ratio. For the diffuser length effect, as mentioned above, the diffuser length is recommended to be between 4 and 8 times the throat diameter. The ejec–tor performance at ($L_4/2r_5 = 2:30$) was numerically predicted at the on-design condition. The effect of dif–fuser lengths on the entrainment ratio is shown in Fig 14, where the results show that the entrainment ratio decreases below ($L_4 / 2r_5 = 4$).

Table 5: Dimensions used for the first optimization

case	Angles		Lengths (mm)					Radii (mm)				$L_3/2r_5$	$L_4/2r_5$
	α	θ	l_1	l_2	l_5	l_6	l_7	r_1	r_2	r_3	r_4		
Opti-1	25	10	40	32.24	18.32	18.32	35.6	6.65	1.32	2.25	11.55	7.5	6

Table 6: Dimensions of optimum geometry

case	Angles		Lengths (mm)					Radii (mm)				$L_3/2r_5$	$L_4/2r_5$
	α	θ	l_1	l_2	l_5	l_6	l_7	r_1	r_2	r_3	r_4		
Opti_2	23	10	40	32.24	18.32	18.32	35.6	6.65	1.32	2.25	11.55	4	6

3.4 Optimum geometry and operating conditions

The above study assisted in establishing important ejector geometry aspects that affect overall performance to produce an optimized geometry of a prechosen case study (model AB1 from Table 3); the optimized dimen–sions are shown in Table 6. For the same inlet con–ditions and at the on-design outlet condition (condenser back pressure under critical value), it was found that the 'entrainment ratio' increased from 0.3935 to 1.2001.

The new optimized model was tested in a variety of operating conditions, as shown in Table 7 and Figure 15.

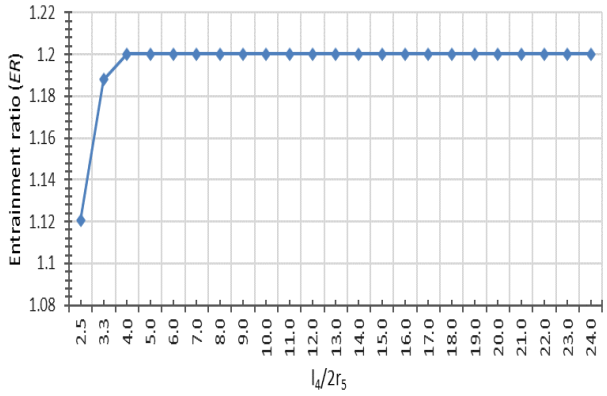

Figure 14: Effect of changing the diffuser section length on the ejector performance

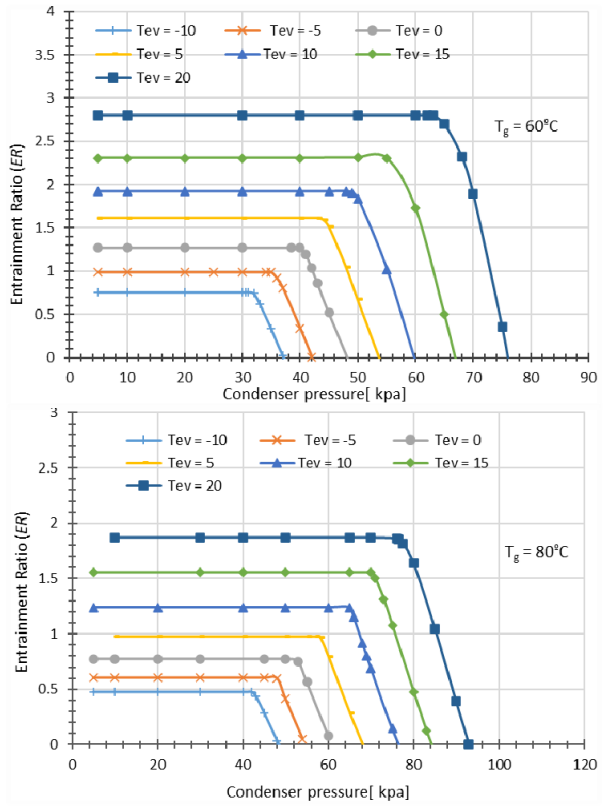

Figure 15: Summary of the new optimized model results at different operating conditions

Table 7: Summary of opti-2 CFD simulation results showing the ejector's entrainment ratio and the critical pressure of the condenser

Evaporator inlet saturation temperature (°C)	Entrainment ratio [critical condenser pressure (kPa)]	
	Generator inlet saturation temperature (°C) / [saturation pressure (kPa)]	
	60°C [264kPa]	80°C [422kPa]
-10	0.758 [31.9]	0.477 [42.5]
-5	0.988 [35.4]	0.606 [47.8]
0	1.272 [40.5]	0.775 [53.0]
5	1.615 [43.0]	0.978 [58.0]
10	1.921 [48.0]	1.238 [65.2]
15	2.308 [55.0]	1.560 [70.0]
20	2.804 [62.0]	1.870 [76.0]

4. CONCLUSIONS

The first section of the paper focused on the validation of a numerical CFD model created using the ansys fluent 18.2 workbench package for simulation, analysis, and design of highly efficient supersonic ejectors for refrigeration applications. The validation was primarily focused on the choice of the more suitable turbulence model in terms of having an acceptable accuracy in the quantitative predictions for primary and secondary mass flow rates (Entrainment ratio) and convergence time. The different turbulence models were then applied to different geometries and operating conditions for experimental investigations. It has been shown that the pressure-based Realizable k-ε model results agreed well with the corresponding experimental results. The largest difference between the pressure-based Realizable k-ε model results and the experimental results was 9 %.

The geometrical parameters, such as angle of convergence, throat section length, and diffuser section (divergence angle and diffuser length), have been optimized, and their effect on entrainment ratio has been investigated. The study's most important conclusions are presented below.

1. The optimal convergence angle was about 23°; increasing or decreasing the angle from that value decreases the ejector performance (entrainment ratio).
2. The optimal length of the throat section is about four times the throat diameter.
3. The divergence angle of the diffuser section is recommended to be from 8° to 15°.
4. The diffuser length is recommended to be larger than 4 times the throat diameter.

The above study assisted in producing an optimized geometry of a prechosen case study where the entrain–ment ratio' increased from 0.3935 to 1.2001 for the same operating conditions.

The performance of the optimized geometry design was predicted over a range of operating conditions.

REFERENCES

[1] E. J. Roschke, P. F. Massier, and H. L. Gier, Experimental investigation of exhaust diffusers for rocket engines. Jet Propulsion Laboratory, California Institute of Technology, 1962.

[2] B. Zhou, B. A. Fleck, F. Bouak, and J. E. D. Gauthier, "Comparison of turbulence models for swirling effects on ejector performances," in 8th Annual Conference of the CFD Society of Canada, 2000, pp. 321–327.

[3] K. Chunnanond and S. Aphornratana, "Ejec–tors: applications in refrigeration technology," Renewable and sustainable energy reviews, vol. 8, no. 2, pp. 129–155, 2004.

[4] S. Da-Wen, I. W. Eames, "Recent developments in the design theories and applications of ejec–tors," J. Inst. Energy, vol. 68, pp. 65–79, 1995.

[5] J. M. Abdulateef, K. Sopian, M. A. Alghoul, and M. Y. Sulaiman, "Review on solar-driven ejector refrigeration technologies," Renewable and Sustainable Energy Reviews, vol. 13, no. 6–7, pp. 1338–1349, 2009.

[6] S. Elbel and P. Hrnjak, "Ejector refrigeration: an overview of historical and present developments with an emphasis on air-conditioning applications," 2008.

[7] S. Elbel, "Historical and present developments of ejector refrigeration systems with emphasis on transcritical carbon dioxide air-conditioning applications," International Journal of Refri–geration, vol. 34, no. 7, pp. 1545–1561, 2011.

[8] X. Chen, S. Omer, M. Worall, and S. Riffat, "Recent developments in ejector refrigeration technologies," Renewable and Sustainable Energy Reviews, vol. 19, pp. 629–651, 2013.

[9] J. H. Keenan and E. P. Neumann, "A simple air ejector," 1942.

[10] B. J. Huang, J. M. Chang, C. P. Wang, V. A. Petrenko, "A 1-D analysis of ejector perfor–mance," International journal of refrigeration, vol. 22, no. 5, pp. 354–364, 1999.

[11] Y. Bartosiewicz, Z. Aidoun, P. Desevaux, Y. Mercadier, "Numerical and experimental in–vestigations on supersonic ejectors," Int J Heat Fluid Flow, vol. 26, no. 1, pp. 56–70, 2005.

[12] Y. Bartosiewicz, Z. Aidoun, Y. Mercadier, "Numerical assessment of ejector operation for refrigeration applications based on CFD," ApplTherm Eng, vol. 26, no. 5–6, pp. 604–612, 2006.

[13] A. E. Ablwaifa, "A theoretical and experi–mental investigation of jet-pump refrigeration system," University of Nottingham, 2006.

[14] V. Zmijanović, B. Rašuo, A. Chpoun, "Flow separation modes and side phenomena in an overexpanded nozzle," *FME Transactions*, vol. 40, no. 3, pp. 111–118, 2012.

[15] Y. Zhu, P. Jiang, "Experimental and numerical investigation of the effect of shock wave characteristics on the ejector performance," International Journal of Refrigeration, vol. 40, pp. 31–42, 2014.

[16] F. Mazzelli, A. Milazzo, "Performance analysis of a supersonic ejector cycle working with R245fa," International journal of refrigeration, vol. 49, pp. 79–92, 2015.

[17] S. Watanawanavet, "Optimization of a high-efficiency jet ejector by computational fluid dynamic software," Texas A&M University, 2005.

[18] R. L. Yadav and A. W. Patwardhan, "Design aspects of ejectors: Effects of suction chamber geometry," Chem Eng Sci, vol. 63, no. 15, pp. 3886–3897, 2008.

[19] Y. Zhu, W. Cai, C. Wen, and Y. Li, "Nume–rical investigation of geometry parameters for design of high performance ejectors," Appl Therm Eng, vol. 29, no. 5–6, pp. 898–905, 2009.

[20] N. Ruangtrakoon, T. Thongtip, S. Aphorn–ratana, and T. Sriveerakul, "CFD simulation on the effect of primary nozzle geometries for a steam ejector in refrigeration cycle," Inter–national Journal of Thermal Sciences, vol. 63, pp. 133–145, 2013.

[21] S. Živković, M. Milinović, and N. Adamec, "Experimental and numerical research of a supersonic planar thrust vectoring nozzle via mechanical tabs," *FME Transactions*, vol. 42, no. 3, pp. 205–211, 2014, doi: 10.5937/fmet1403205Z.

[22] O. P. Kostić, Z. A. Stefanović, I. A. Kostić, "CFD modeling of supersonic airflow gene–rated by 2D nozzle with and without an obstacle at the exit section," *FME Transac–tions*, vol. 43, no. 2, pp. 107–113, 2015, doi: 10.5937/fmet1502107K.

[23] S. K. Yadav, K. M. Pandey, R. Gupta, and V. Kumar, "Numerical study for the influences of nozzle exit position, mixing, and diffuser section lengths on performance of CRMC ejector," Journal of the Brazilian Society of Mechanical Sciences and Engineering, vol. 43, no. 11, pp. 1–14, 2021.

[24] S. Luis Tolentino and J. Mirez, "Throat Length Effect on the Flow Patterns in Off-Design Conical Nozzles," *FME Transactions*, vol. 50, no. 2, pp. 271–282, 2022, doi: 10.5937/fme2201271T.

[25] B. El Zohbi, N. Bukharin, H. H. Assoum, K. Abed-Meraim, A. Sakout, and M. El Hassan, "Investigation of the effects of the jet nozzle geometry and location on the performance of supersonic fluid ejectors," Energy Reports, vol. 8, pp. 228–233, 2022.

[26] U. D. F. Manual, "ANSYS FLUENT 12.0," *Theory Guide*, p. 67, 2009.

[27] J. Bredberg, "On the wall boundary condition for turbulence models," Chalmers University of Technology, Department of Thermo and Fluid Dynamics. Internal Report 00/4. G oteborg, pp. 8–16, 2000.

[28] D. Scott, Z. Aidoun, O. Bellache, M. Ouzzane, "CFD simulations of a supersonic ejector for use in refrigeration applications," 2008.

[29] A. F. U. Guide, “Release 18.2, 2017 ANSYS.” Inc.

[30] A. D. Third, I) The Air Ejector. II) Recom–pression Losses in The Divergent Nozzle. Uni–versity of Glasgow (United Kingdom), 1928.

[31] F. R. B. Watson, “The production of a vacuum in an air tank by means of a steam jet,” Pro–ceedings of the Institution of Mechanical Engi–neers, vol. 124, no. 1, pp. 231–300, 1933.

[32] A. E. Kroll, “The design of jet pumps,” Chem Eng Prog, vol. 43, no. 1, pp. B21–B24, 1947.

[33] R. B. Engdahl and W. C. Holton, “A General Method of Designing Gas and Gas-Liquid Injectors Using Laws of Turbulent Jet Mixing,” J. Appl. Mech. Trans. ASME, vol. 65, 1943.

[34] P. A. Bhat, A. K. Mitra, A. N. Roy, “Momen–tum transfer in a horizontal liquid-jet ejector,” Can J Chem Eng, vol. 50, no. 3, pp. 313–317, 1972.

[35] J. Zahradnik, F. Kaštánek, J. Kratochvil, and M. Rylek, “Hydrodynamic characteristics of gas-liquid beds in contactors with ejector-type gas distributors,” Collect Czechoslov Chem Commun, vol. 47, no. 7, pp. 1939–1949, 1982.

[36] M. Moresi, G. BartoloGianturco, and E. Sebastiani, “The ejector-loop fermenter: description and performance of the apparatus,” BiotechnolBioeng, vol. 25, no. 12, pp. 2889–2904, 1983.

[37] A. Ben Brahim, M. Prevost, and R. Bugarel, “Momentum transfer in a vertical down flow liquid jet ejector: case of self gas aspiration and emulsion flow,” International journal of multi–phase flow, vol. 10, no. 1, pp. 79–94, 1983.

[38] S. R. Bhutada, V. G. Pangarkar, “Gas induc–tion and hold-up characteristics of liquid jet loop reactors,” Chem Eng Commun, vol. 61, no. 1–6, pp. 239–258, 1987.

[39] G. Kundu, D. Mukherjee, A. K. Mitra, “Gas entrainment and depth of penetration in a co-current gas-liquid downflow bubble column,” Journal of chemical engineering of Japan, vol. 27, no. 5, pp. 621–626, 1994.

[40] P. Havelka, V. Linek, J. Sinkule, J. Zahradnik, M. Fialova, “Effect of the ejector configuration on the gas suction rate and gas hold-up in ejector loop reactors,” Chem Eng Sci, vol. 52, no. 11, pp. 1701–1713, 1997.

[41] P. Cramers and A. Beenackers, “Influence of the ejector configuration, scale and the gas density on the mass transfer characteristics of gas–liquid ejectors,” Chemical Engineering Journal, vol. 82, no. 1–3, pp. 131–141, 2001.

[42] A. Elgozali, V. Linek, M. Fialová, O. Wein, and J. Zahradnk, “Influence of viscosity and surface tension on performance of gas–liquid contactors with ejector type gas distributor,” Chem Eng Sci, vol. 57, no. 15, pp. 2987–2994, 2002.

[43] X. Gamisans, M. Sarrà, and F. J. Lafuente, “Fluid flow and pumping efficiency in an ejector-venturi scrubber,” Chemical Enginee–ring and Processing: Process Intensification, vol. 43, no. 2, pp. 127–136, 2004.

[44] E. Rusly, L. Aye, W. W. S. Charters, A. Ooi, “CFD analysis of ejector in a combined ejector cooling system,” International Journal of Ref–rigeration, vol. 28, no. 7, pp. 1092–1101, 2005.

[45] M. Li, P. D. Christofides, “Multi-scale modeling and analysis of an industrial HVOF thermal spray process,” Chem Eng Sci, vol. 60, no. 13, pp. 3649–3669, 2005.

[46] K. Banasiak, A. Hafner, and T. Andresen, “Experimental and numerical investigation of the influence of the two-phase ejector geometry on the performance of the R744 heat pump,” International journal of Refrigeration, vol. 35, no. 6, pp. 1617–1625, 2012.

[47] S. Varga, A. C. Oliveira, B. Diaconu, “Inf–luence of geometrical factors on steam ejector performance–a numerical assessment,” Inter–national journal of refrigeration, vol. 32, no. 7, pp. 1694–1701, 2009.

[48] D. Scott, Z. Aidoun, M. Ouzzane, “An expe–rimental investigation of an ejector for validating numerical simulations,” Inter–national journal of refrigeration, vol. 34, no. 7, pp. 1717–1723, 2011.

[49] D. A. Scott, Z. Aidoun, “CFD analysis of an ejector for cooling applications,” in The 23rd IIR International Congress of Refrigeration, Prague, 2011.

[50] B. Zhang, X. Song, J. Lv, J. Zuo, “Study on the key ejector structures of the waste heat-driven ejector air conditioning system with R236fa as working fluid,” Energy Build, vol. 49, pp. 209–215, 2012.

[51] J. Yan, W. Cai, Y. Li, "Geometry parameters effect for air-cooled ejector cooling systems with R134a refrigerant," Renew energy, vol. 46, pp. 155–163, 2012.

[52] S. Elbel, P. Hrnjak, “Experimental validation of a prototype ejector designed to reduce throttling losses encountered in transcritical R744 system operation,” International Journal of Refrigeration, vol. 31, no. 3, pp. 411–422, 2008.

[53] K. Banasiak, A. Hafner, and T. Andresen, “Experimental and numerical investigation on R744 ejector geometry,” in The 23th IIR International Congress of Refrigeration, 2011.

NOMENCLATURE

H	specific enthalpy (kJ/kg)
T	temperature ($^{\circ}$C)
L	lengths of the ejector in the z-direction (mm)
p	pressure (kPa)
z	axial direction
r	radial direction

Greek symbols

ρ	density
α	angle of the convergent section of the ejector
θ	angle of the divergent section of the ejector

Subscripts

g_{gen}	saturated vapor at the generator temperature
g_{evap}	saturated vapor at the evaporator temperature
f_{con}	saturated liquid at the condenser temperature
E	Secondary entrained flow from the evaporator
g	primary flow from the generator

Superscripts

c*	critical point

Abbreviations

ER	entrainment ratio of an ejector
cop	coefficient of performance

ЦФД АНАЛИЗА И ИСПИТИВАЊЕ ГЕО–МЕТРИЈСКИХ ПАРАМЕТАРА ЗА ДИЗАЈН ВИСОКОЕФИКАСНОГ НАДЗВУЧНОГ ЕЈЕКТОРА

М. Елгезар, А. Рашад, М.С. Хасан, Т. Елнади

Овај рад представља ЦФД анализу модела суперсоничног ејектора за расхладне системе. Модел је потврђен поређењем са претходним сту–дијама и коришћен је за пројектовање висо–коефикасног избацивача. Проучавају се ефекти геометријских параметара као што су угао конвергенције, дужина грла, угао дивергенције и дужина дифузора на однос увлачења. Оптималне вредности ових параметара се проналазе и користе за модификовање основног модела. Перформансе оптимизованог модела се процењују у различитим условима рада. Рад има за циљ да пружи смернице за дизајн суперсоничних ејектора у расхладним апликацијама